

Extra-axial brain tumours and cysts

Maria Politi^{1,2}, Kirill Alektorov², Lia Angela Moulopoulos³, Panagiotis Papanagiotou^{2,3}

¹Neuroradiology Section, Affidea Greece

²Department of Diagnostic and Interventional Neuroradiology, Hospital Bremen-Mitte, Germany

³1st Department of Radiology, School of Medicine, National and Kapodistrian University of Athens, Areteion Hospital, Athens, Greece

SUBMISSION: 7/6/2020 - ACCEPTANCE: 19/8/2020

ABSTRACT

Extra-axial brain tumours are the most common adult intracranial neoplasms and include a broad spectrum of pathologic subtypes. Meningiomas are the most common extra-axial brain tumours. They may occasionally be difficult to differentiate from other dural-based masses with more aggressive biologic behaviour (e.g. haemangiopericytoma or dural-based metastases). When the mass is located in the cerebel-

lopontine angle, schwannoma is the most common neoplasm, followed by meningioma and epidermoid cyst. Magnetic resonance imaging narrows the differential diagnosis and provides guidance for patient management. This pictorial essay describes the radiographic features of extra-axial lesions and provides an overview of the most common types of extra-axial tumours and their typical imaging features.



KEY WORDS

Brain tumours; CT; MRI; Meningioma; Schwannoma; Epidermoid



CORRESPONDING AUTHOR, GUARANTOR

Maria Politi, MD, PhD
Neuroradiology Section, Affidea Greece, Leof. Kifisias 190, Kifisia 145 62
Department of Diagnostic and Interventional Neuroradiology, Hospital
Bremen-Mitte, Germany. Email: mariapoliti@hotmail.com

Differentiation between extra-axial and intra-axial lesions

Differentiation between extra-axial and intra-axial lesions is important for the diagnosis of the tumour type and is also relevant for surgical planning. Usually this differentiation is straightforward; however, when the mass is large and associated with parenchymal changes, such as oedema, localisation can be more difficult. A number of features are helpful in diagnosing an extra-axial location [1, 2]:

- Subarachnoid space

A well-defined space separates the extra-axial mass from the brain, creating the cerebrospinal fluid (CSF) cleft sign. The brain drifts away from the bone or dura, which can lead to dilated cisterns and widening of adjacent subarachnoid space. Intervening pial arteries or veins are observed.

- Brain parenchyma

Extra-axial lesions generally shift brain structures instead of infiltrating them (absence of "claw" sign). The white matter "buckling" sign is caused by the white matter of the gyri being compressed and displaced by the mass, even in the presence of oedema. Intervening cortex between mass and white matter may be observed. There is usually little or no perifocal oedema.

- Bone and meninges

Thickening of the adjacent dura on both sides of the tumour may occur in addition to the observation of linear contrast enhancement, the so-called "dural tail" sign. Erosion, invasion or destruction of adjacent bone or hyperostosis may be observed.

Supratentorial extra-axial neoplasms occur in several general locations: 1. skull and meninges; 2. CSF spaces (subarachnoid cisterns and ventricles); 3. sella and parasellar region; 4. pineal region [3]. In this article we focus on lesions that involve the skull and its linings.

The most frequent extra-axial neoplasms or cysts are meningiomas, schwannomas, arachnoid cysts, dermoid and epidermoid cysts, and extra-axial metastases.

Meningiomas

Meningiomas originate from arachnoid cap cells, are usually slow-growing and cause displacement, especially of the brain parenchyma. In functionally less relevant locations, these tumours can often reach an impressive size. In contrast, very flat tumours can become symp-

Table 1. List of the different meningioma subtypes based on WHO grading and the likelihood of recurrence [5, 6].

Meningioma	WHO grading
Meningiomas with low risk of aggressive growth and recurrence	
Meningothelial	WHO grade I
Fibrous (fibroblastic)	WHO grade I
Transitional	WHO grade I
Psammomatous	WHO grade I
Angiomatous	WHO grade I
Microcystic	WHO grade I
Secretory	WHO grade I
Lymphoplasmacyte-rich	WHO grade I
Metaplastic	WHO grade I
Meningiomas with increased probability of aggressive growth and/or recurrence	
Atypical	WHO grade II
Clear cell	WHO grade II
Chordoid	WHO grade II
Rhabdoid	WHO grade III
Papillary	WHO grade III
Anaplastic	WHO grade III

tomatic in critical regions. Intracerebral meningiomas are very rare and are almost always located within the ventricular system. Intraosseous meningiomas are very rare.

Epidemiology and aetiology

Meningiomas account for approximately 24-30% of the total number of brain tumours in the United States. The number of cases ranges between 1.6 and 13 per 100,000 population, excluding cases found at autopsy. Their incidence increases with age, with 1.4% of patients at an autopsy series [4] diagnosed with asymptomatic meningioma. In contrast, asymptomatic meningiomas detected at autopsy in individuals aged under 30 years are

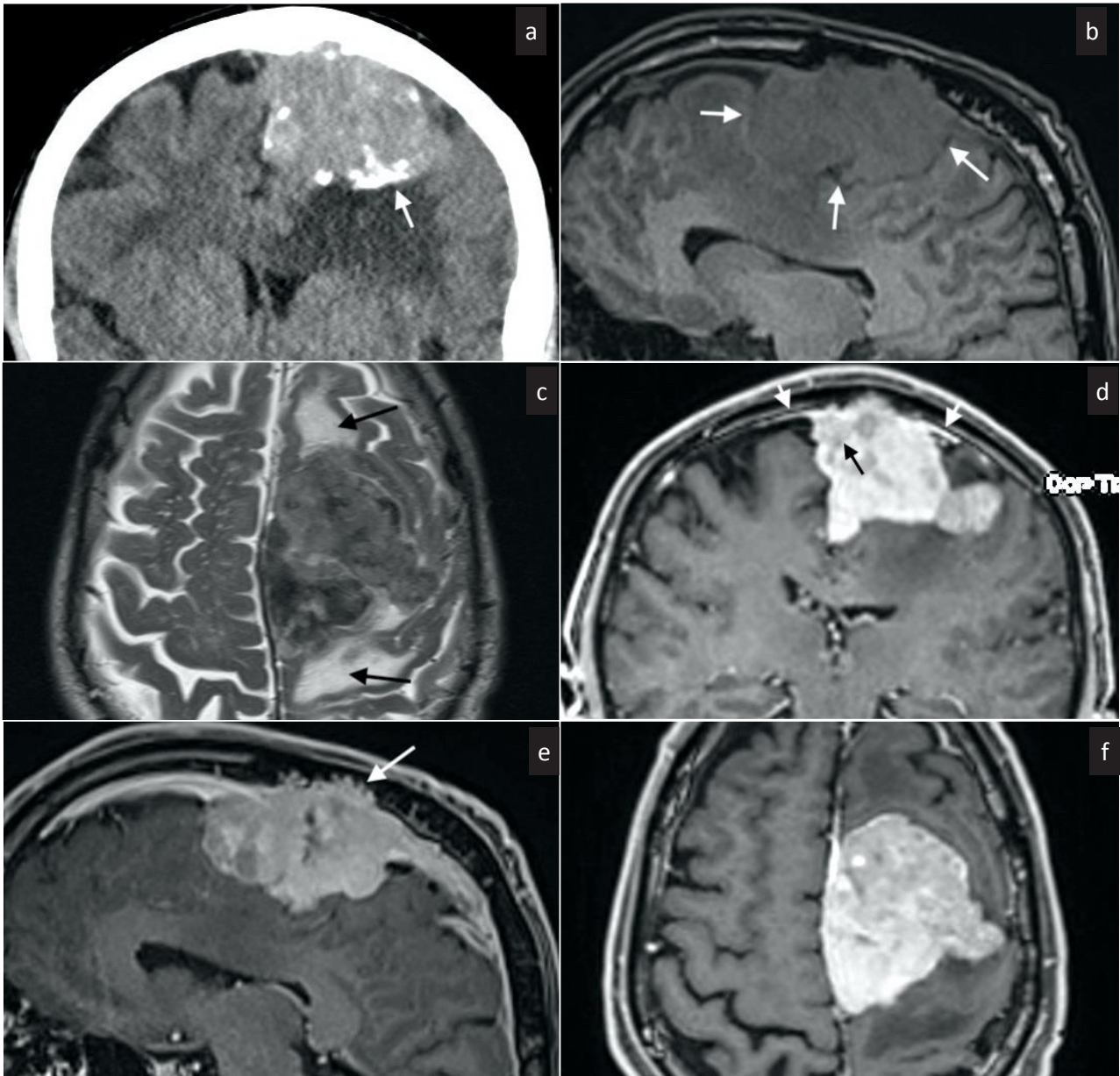


Fig. 1. Large meningioma in a 79-year-old male patient presenting with aphasia and right-sided hemiparesis. Initial non-enhanced CT scan showed a hyperdense, partially calcified mass with compression of the left frontal lobe (arrow in a). MRI demonstrates a T1-isointense tumour (arrows in b) with inhomogeneous low T2-signal and adjacent white matter oedema (arrows in c). Contrast-enhanced T1W Gradient Echo MR images (d-f) show a strongly enhancing mass with a “dural tail”-sign (white arrows in d) and infiltration of the calvaria (arrow in e). The tumour also invades the superior sagittal sinus (black arrow in d).

extremely rare. If a meningioma is diagnosed in a child, neurofibromatosis type II should be considered. They usually occur at an advanced age, with a peak incidence during the sixth decade of life for males and the seventh decade for women. Meningiomas affect women at a rate of 1.5 to 3 times more than men.

The aetiology of meningiomas is largely unknown. However, it is known that they occur more frequently following neurocranial radiation [4, 5].

Classification and grading of meningiomas

Meningiomas develop through the neoplastic transfor-

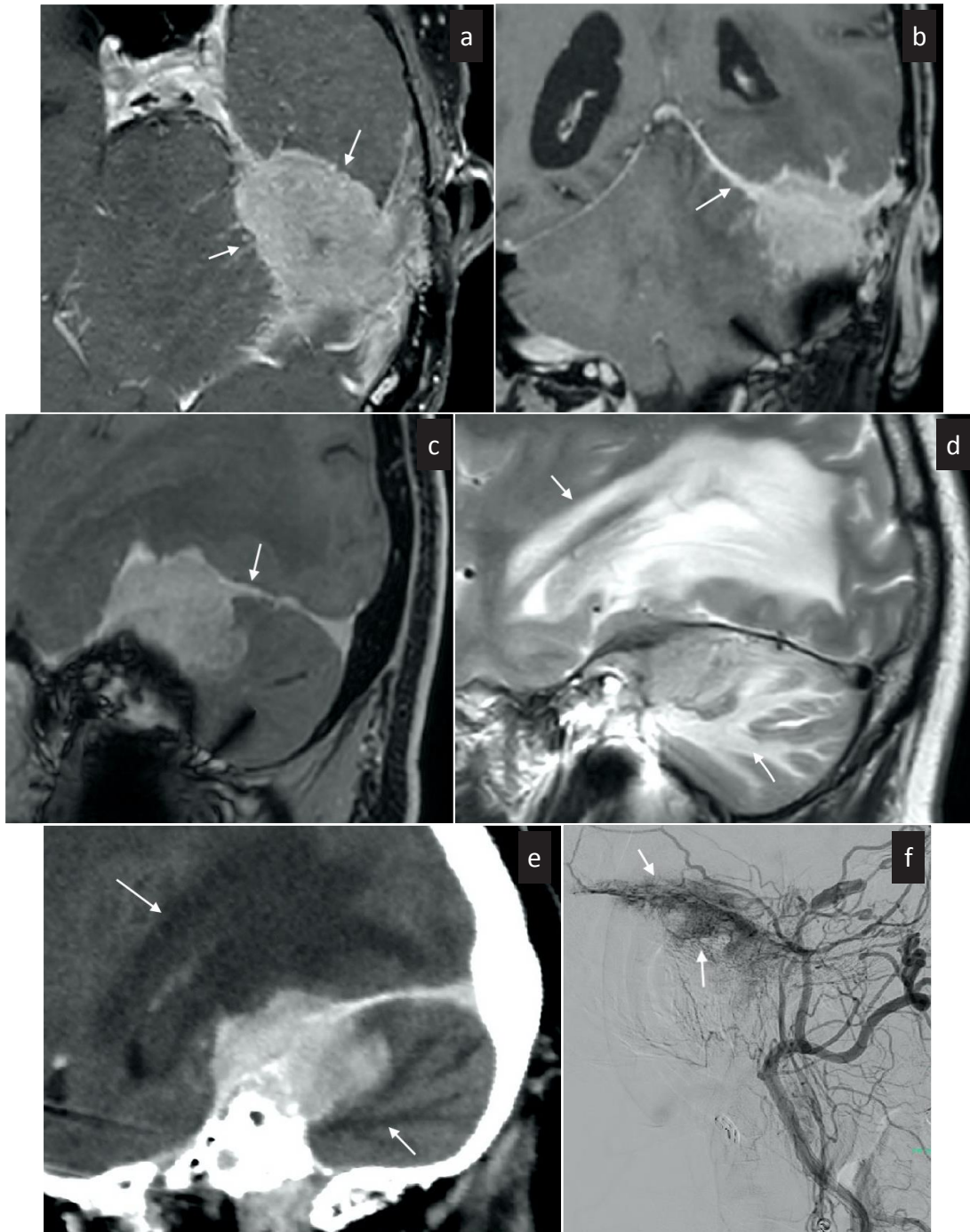


Fig. 2. Atypical meningioma (WHO II) of the left cerebellar tentorium in a 70-year-old patient with vertigo. Contrast-enhanced T1W MR images (a-c) demonstrate a large tumour mass (arrows) in the cerebellar tentorium with irregular margins, strong contrast enhancement and a “dural-tail-sign” (arrow in b). Sagittal T2W MR image (d) and contrast-enhanced CT (e) show extensive oedema of the surrounding supratentorial and cerebellar tissue (arrows). DSA (f) demonstrates a vascular “blush” and arterial tumour supply from the middle meningeal artery (arrows).

mation of meningeal cells and primarily demonstrate a broad-based attachment to the dura mater. Macro-

scopically they usually are well-defined, encapsulated tumours, and have a firm to rubbery consistency. Ex-

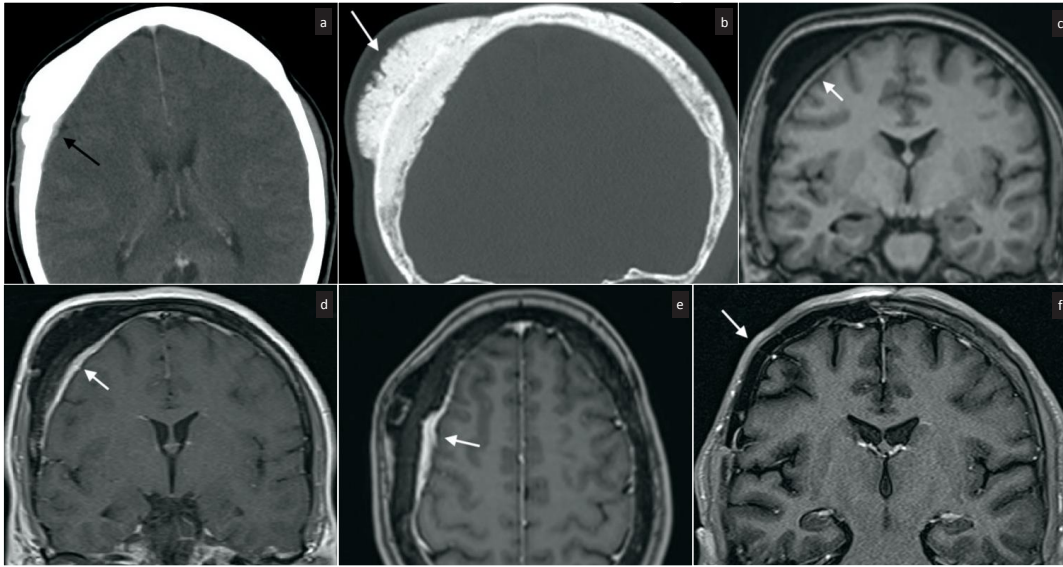


Fig. 3. CT and MRI scans of a 52-year-old female with a slowly growing subcutaneous cranial mass. Contrast-enhanced CT image (a) shows focal thickening of the right frontal calvaria with underlying dural enhancement (arrow). Coronal CT with bone window (b) demonstrates marked hyperostosis of the right frontal bone with irregular margins (arrow). T1W Gradient Echo MRI (c) shows thickening of the right-sided dura (arrow in c) with avid enhancement (arrows in d, e). Surgical resection of the lesion was performed with specimen histology revealing an intraosseous meningioma (WHO I). Postoperative contrast-enhanced T1W MR image (f) showing a hypointense calvarial implant (arrow).

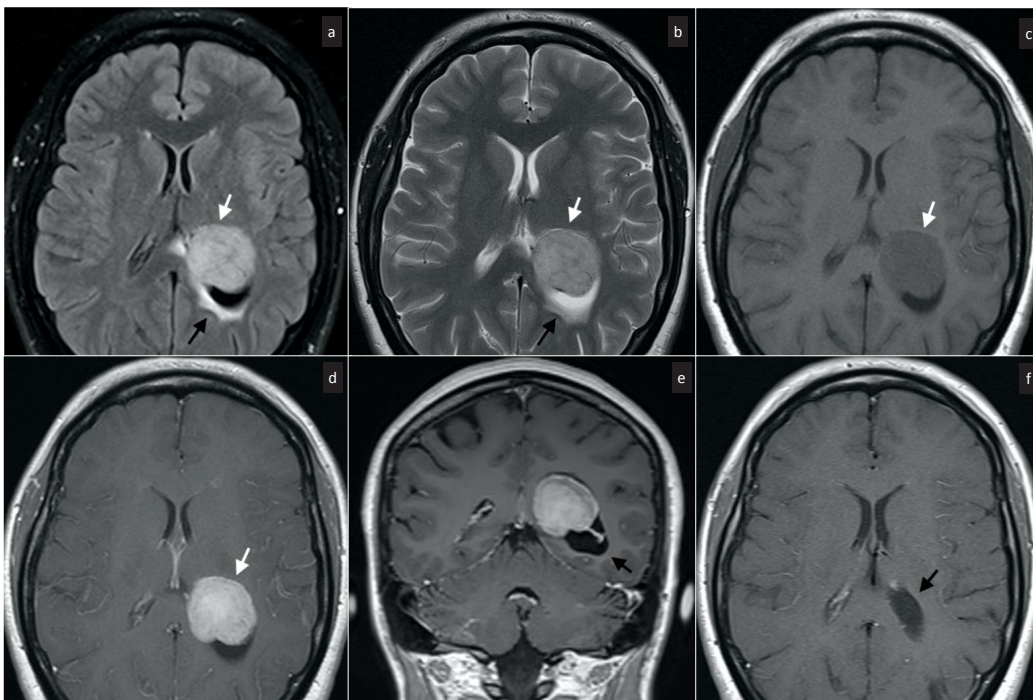


Fig. 4. Intraventricular meningioma in a 36-year-old female patient with recurrent vertigo attacks and headaches. A circumscribed mass in the trigone of the left lateral ventricle with signal intensity isointense to gray matter on FLAIR and T2W MR images (white arrows in a and b). The tumour caused dilatation of the posterior and temporal horn with resulting fluid diapedesis (black arrows in a and b). The lesion shows isointense to gray matter signal on T1W MR images (arrow in c) and strong enhancement on contrast-enhanced T1W MR images (arrows in d, e). After complete tumour resection, residual dilatation of the posterior left horn can still be observed (arrow in f).

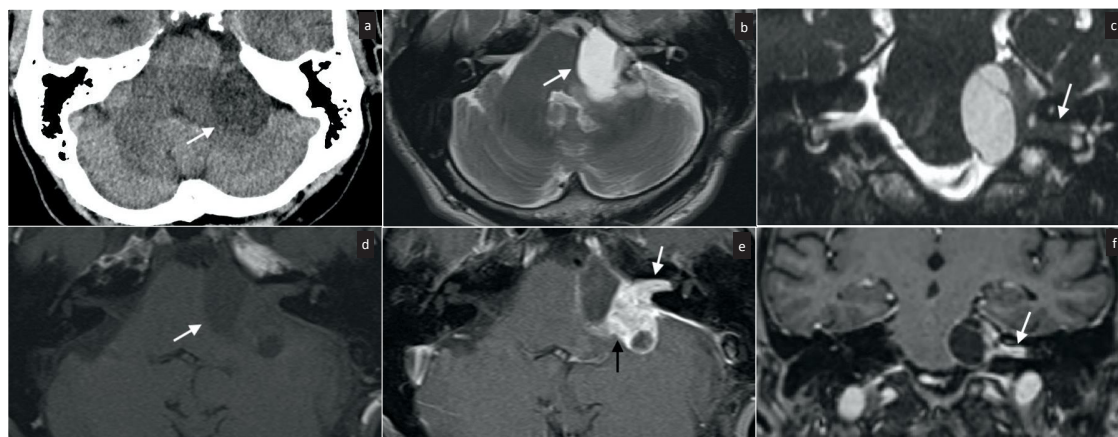


Fig. 5. Vestibular nerve schwannoma in a 62-year-old male patient with nausea and vertigo. Non-enhanced CT (a) scan and T2W MR images (b, c) demonstrate a partially cystic mass in the left CPA with compression of brainstem and cerebellum (arrows). The solid component of the mass shows T2-hypointense signal, extending into the internal auditory canal (arrow in c). T1W (d) and contrast-enhanced T1W (e, f) MR images, demonstrate a mass with a hypointense cystic component and marked enhancement of the solid tumour parts (arrows).

ceptions are the rare microcystic and mucinous meningiomas, which are soft. The cross-sectional surface is grayish-white, often lobulated, and may be granular due to calcification. The tumour compresses and displaces surrounding brain tissue. However, the border to the brain parenchyma remains sharply defined in World Health Organisation (WHO) grade I benign meningiomas. After tumour removal, a depressed bed is left behind in the brain.

Meningiomas exhibit a highly variable histopathological appearance, with WHO recognising 15 variations, including nine histological subtypes of benign meningiomas (Table 1) [5, 6].

Meningiomas (WHO grade I)

The different WHO grade I meningioma variants are listed in Table 1. However, it is not uncommon to find differentiated areas in a tumour that are morphologically variable. If systematic subtyping is performed, the subtype is determined according to the predominant growth form, whereby mixed forms with both meningotheelial and fibroblastic differentiation features are classified as transitional meningiomas.

Meningiomas (WHO grade II)

In addition to grade I meningioma variants, certain histological subtypes exhibit aggressive growth and a tendency to local recurrence after surgical removal, without being classical malignant tumours (Table 1). These

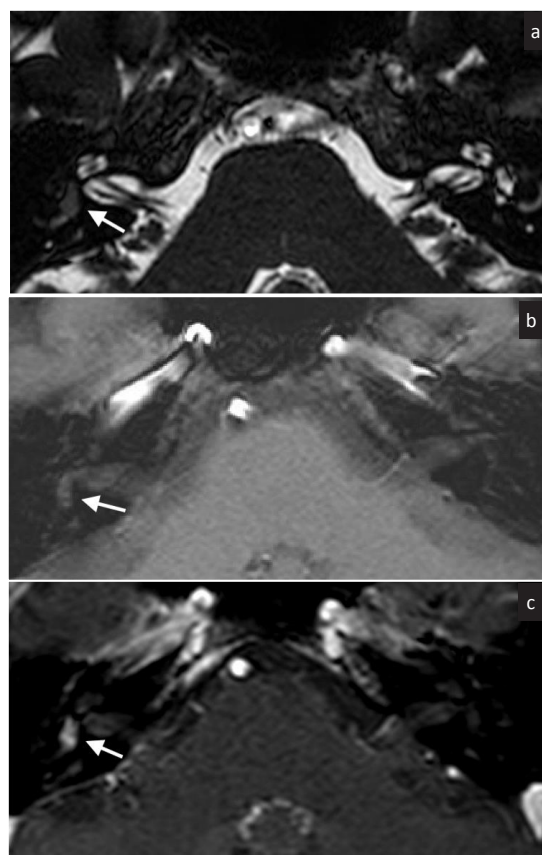


Fig. 6. Small intralabyrinthine schwannoma in a 36-year-old female patient with tinnitus and hearing loss. Thin-slice T2*W MR image of the CPA shows a hypointense nodular mass in the vestibulum of the right labyrinth (arrow in a). The lesion is T1-isointense to brain parenchyma (arrow in b) and demonstrates intense nodular contrast enhancement on T1W contrast-enhanced MR image (arrow in c).

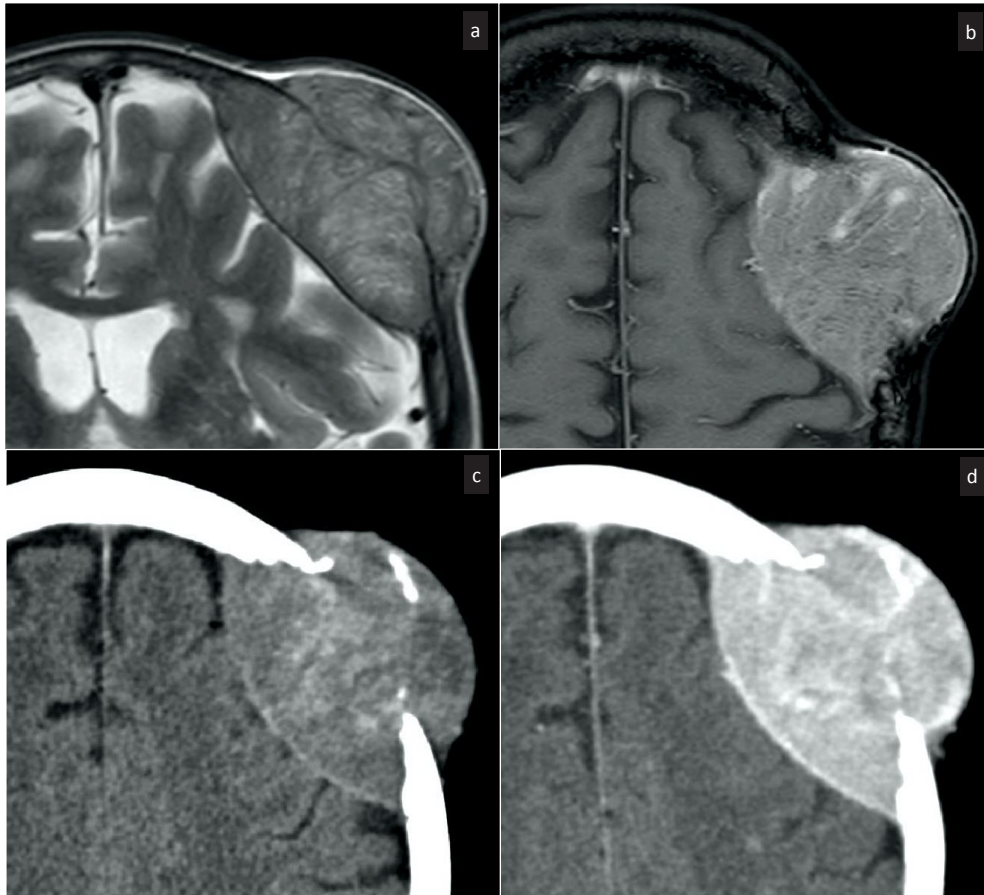


Fig. 7. Large skull metastasis in a 60-year-old patient with a history of hepatocellular carcinoma, presenting with a new subcutaneous mass. T2W and contrast-enhanced T1W MR images (a, b) as well as plain CT (c) and contrast-enhanced CT (d) scans demonstrate a heterogeneous soft tissue mass with extensive destruction of the frontal calvarium and protrusion into the epidural space. The lesion shows strong contrast enhancement on both CT and MRI (b, d).

are classified as WHO grade II meningiomas. In the 2016 classification, brain invasion joins a mitotic count of 4 or more as a histological criterion that can alone suffice for diagnosing an atypical meningioma, WHO grade II [7]. Atypical meningioma can also be diagnosed on the basis of the additive criteria of 3 of the other 5 histological features: spontaneous necrosis, sheeting (loss of whorling or fascicular architecture), prominent nucleoli, high cellularity and small cells (tumour clusters with high nuclear:cytoplasmic ratio).

Meningiomas (WHO grade III)

Finally, there is also a small group of meningiomas (approximately 2-3% of all meningiomas) that exhibit histologic anaplasia and are characterised by invasive

and destructive growth as well as the potential to metastasise. This rare group of malignant meningiomas includes three different variants (**Table 1**).

Schwannomas

Schwannomas are benign tumours arising from Schwann cells. They form within the myelin sheath around the axons of nerve fibres. Schwannomas constitute approximately 8% of all primary brain tumours. They are more common in adults. In adults, 90% of extra-axial CPA tumours are schwannomas, followed by meningiomas (10-15%). Schwannomas account for approximately 2% of tumours in the posterior fossa in children. If a schwannoma is diagnosed in a child, neurofibromatosis type II should be considered. Other

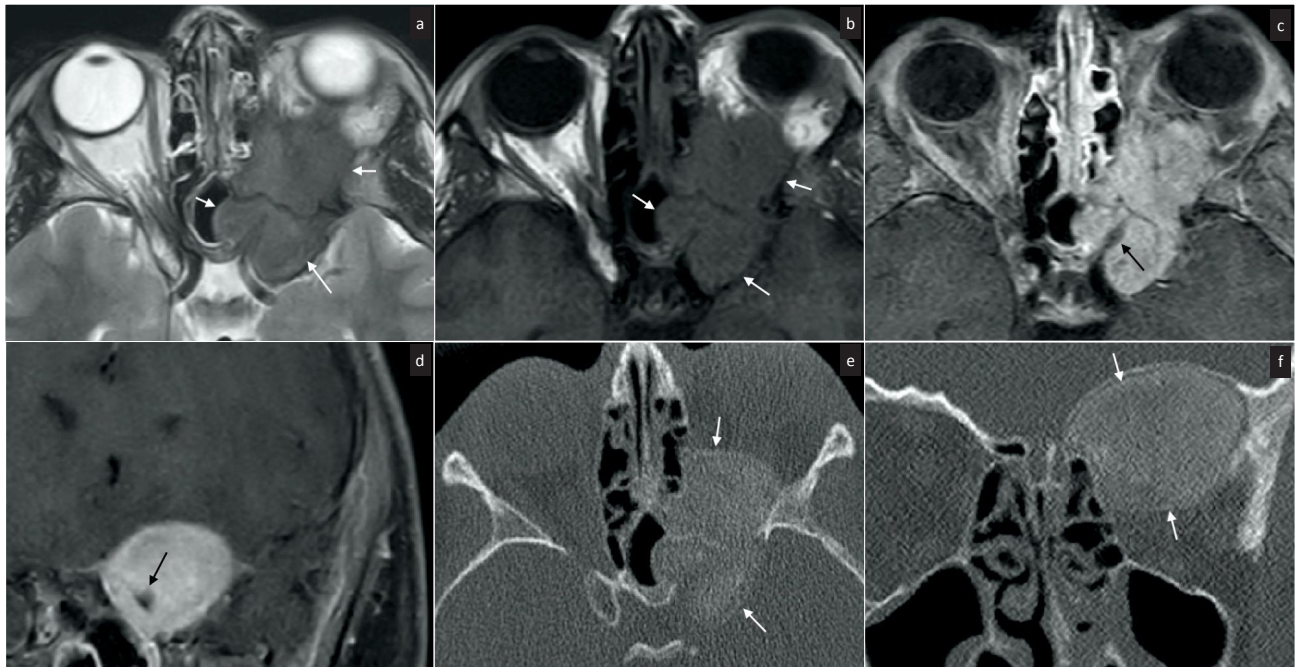


Fig. 8. Ossifying fibroma of the orbit and frontal skull base in a 13-year-old patient with exophthalmos and vision loss. T2W and T1W MR images (a, b) show a hypointense mass (arrows) infiltrating the orbital apex, with intense contrast enhancement on contrast-enhanced T1W MR images (c, d). The tumour completely encases the optic nerve (black arrows in c, d) as seen on axial and coronal images. Non-enhanced CT scan demonstrates homogeneous ground-glass tumour density (arrows in e, f).

schwannomas and meningiomas should also be looked for.

In 95% of cases, schwannomas affect the vestibular part of the eighth cranial nerve, the vestibulocochlear nerve. Non-vestibular schwannomas account for 5% of all cases, with cranial nerves V, IX, and X most frequently affected. Vestibular schwannomas often occur in the internal auditory canal or the CPA. If a vestibular schwannoma grows and expands into the CPA, symptoms occur as a result of pressure on the adjacent neural structures. Signs of brainstem compression or hydrocephalus often occur as a result of compression of the aqueduct or the 4th ventricle [11, 12].

Imaging

On CT, schwannomas appear hypo- or isodense. Central necrosis can occur in large tumours. After contrast administration, homogeneous enhancement is typically observed. Tumour growth within the internal auditory canal leads to expansion within the petrous portion of the temporal bone. These lesions often cannot be diagnosed by CT [13, 14].

On MRI, schwannomas usually appear isointense to brain parenchyma. Larger tumours often show heterogeneous signal on T2-weighted (T2W) images with areas of high and low signal intensity (Fig. 5). These hypointense areas are frequently caused by intratumoural haemorrhage. Cranial nerve thickening is usually marked by an enlarged neural foramen, e.g., the foramen ovale and foramen rotundum in trigeminal schwannomas and the internal auditory canal in vestibular schwannomas. Moreover, after administration of contrast they demonstrate intense, primarily homogeneous enhancement.

Intrameatal vestibular schwannomas are evident on T2W MR images due to loss of fluid signal intensity of the internal auditory canal. On CT, enlargement of the internal auditory canal within the petrous part of the temporal bone may be observed. The tumour enhances homogeneously after the administration of contrast agent. Large vestibular schwannomas extend into the CPA, resulting in a characteristic image of an “ice cream cone” appearance. Furthermore, larger lesions often contain intratumoural cysts and areas of necro-

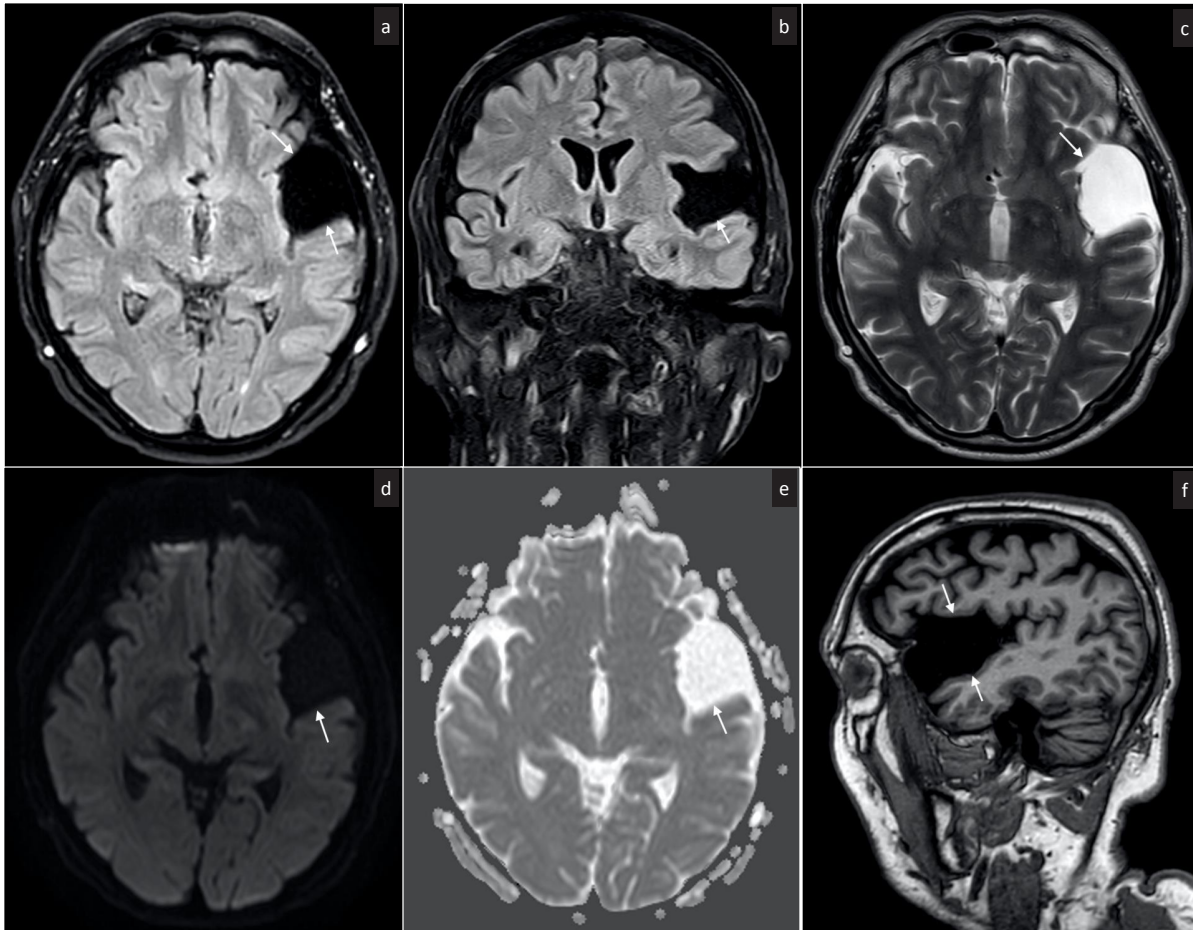


Fig. 9. Arachnoid cyst as an incidental finding in a 66-year-old male patient with a history of epileptic seizures. The MR images show a cystic mass in the left temporal fossa with impression of the frontal and temporal lobe. The lesion is isointense to CSF-signal in the FLAIR and T2W spin echo sequences (arrows in a-c) and shows no restricted diffusion (arrows in d, e). The T1W Gradient Echo MR image shows a CSF-isointense mass with distention of the Sylvian fissure (arrow in f).

sis (**Fig. 5**). Important differentiating criteria between a vestibular schwannoma and a meningioma are a dural tail sign and a broad-based dural attachment, both present in meningiomas. The internal auditory canal is usually not affected in meningiomas, i.e. there is no tumour growth in this area. Intratumoural calcifications are rare in schwannomas and indicate the presence of a meningioma [11, 13, 14].

Vestibular or cochlear schwannomas may be localised in the vestibulum. They are often small lesions that can be easily overlooked. On T2W sequences, there is loss of the fluid signal in the affected segment. In such cases, high-resolution 3D sequences, such as CISS are useful. Lesions are evident on contrast-enhanced images (**Fig. 6**). On plain T1W MR images, the tumour is

hypointense and, therefore, can be differentiated from intralabyrinthine haemorrhage, which is hyperintense [15, 16].

Trigeminal schwannomas can affect any segment of the trigeminal nerve including the cisternal segment of the CPA, Meckel's cave, cavernous sinus, and inferior orbital fissure. Trigeminal schwannomas usually have a dumbbell appearance, caused by two components of the tumour, the infratentorial part at the medial CPA and the supratentorial part at Meckel's cave.

Jugular foramen schwannomas affect the glossopharyngeal nerve. These tumours cause an enlarged jugular foramen with a sclerotic margin without bony erosion or osteolysis. They extend from the posterior cranial fossa through the jugular foramen beyond the

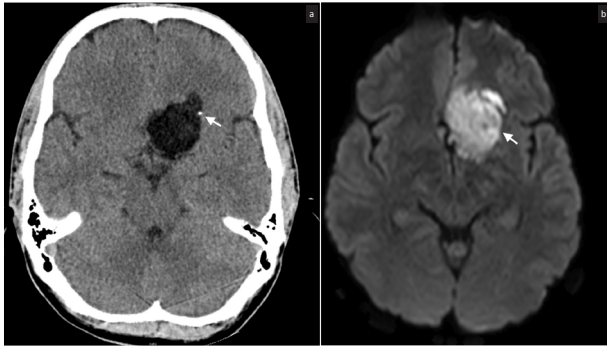


Fig 10. Patient with an epidermoid cyst. Non-enhanced CT scan (a) shows a hypodense cystic mass in the left frontal region, with a small calcification (arrow). Diffusion restriction of the mass on the high b value DWI-MR image (arrow in b) is a typical sign of epidermoid cysts.

base of the skull into the parapharyngeal space.

Facial nerve schwannomas can occur in the CPA, middle ear, geniculate ganglion, as well as the facial canal. These tumours can widen the facial canal and often cause temporal bone erosion [13-16].

Haemangiopericytoma

This rare tumour arises from primitive mesenchymal cells throughout the body. It represents less than 1% of primary central nervous system (CNS) tumours and occurs in the 4th-6th decade, with the mean age of patients being 43 years. It is a WHO grade II and III tumour, with high cellularity and vascularity and a tendency to bleed at surgery.

It is seen as a lobular, well-circumscribed, encapsulated firm, extra-axial mass with dural attachment that mimics meningioma. Typically it is located above the tentorium in the occipital region and it often involves the tentorium, the falx and the dural sinuses. Unlike meningiomas, it does not have any calcifications nor does it cause hyperostosis, however it often causes skull erosion. On T1- and T2W MR sequences it is seen as a heterogeneous isointense mass, with prominent flow voids and surrounding oedema. After intravenous injection of contrast agent it shows strong enhancement, often heterogeneous, with a dural-tail sign seen in 50% of the cases.

The treatment of choice is surgical resection with radiation therapy or radiosurgery to reduce the risk of

local recurrence. Because the tumours are highly vascular, preoperative embolisation may be helpful. Extracranial metastases to the liver, lungs, lymph nodes and bones occur in up to 30% of patients and 5-year survival rate is up to 93% [17].

Metastases

Metastases are the second most common extra-axial neoplasms. They can be skeletal (bone), dural, or leptomeningeal.

Bone metastases are primarily due to primary neoplasms of the lung, breast, and prostate. In children, metastatic neuroblastoma can affect the skull. These can be diagnosed on CT images viewed on bone window. MRI better depicts extension of metastases to the epidural space and involvement of the dura mater (**Fig. 7**).

Dural metastases without bone involvement are rare and most often associated with prostate cancer and malignant melanoma. The differential diagnosis between dural metastases and meningiomas can be challenging. Oedema in the adjacent brain parenchyma is frequently present in metastases but can also occur in meningiomas. A history of malignant disease plays an important role.

Leptomeningeal metastases, also called meningeal carcinomatosis, can be detected on MRI. Contrast-enhanced T1W MR sequences show enhancement in the subarachnoid space of the cisterns, fissures, and cortical sulci [18-22].

Bone tumours

Different primary bone tumours located at the skull, including chordoma, which is primarily located in the skull base, eosinophilic granuloma, multiple myeloma, bone haemangioma, ossifying fibroma (**Fig. 8**), Ewing sarcoma, and osteosarcoma may also be associated with epidural masses [20, 23].

Arachnoid cysts

Arachnoid cysts are circumscribed cysts filled with CSF covered by arachnoid membrane with no communication with the ventricular system. Their location can be supratentorial, commonly in the middle cranial fossa, or infratentorial in the posterior fossa. In most cases, they are incidental findings and do not cause symptoms. Arachnoid cysts can become symptomatic when the lesion is

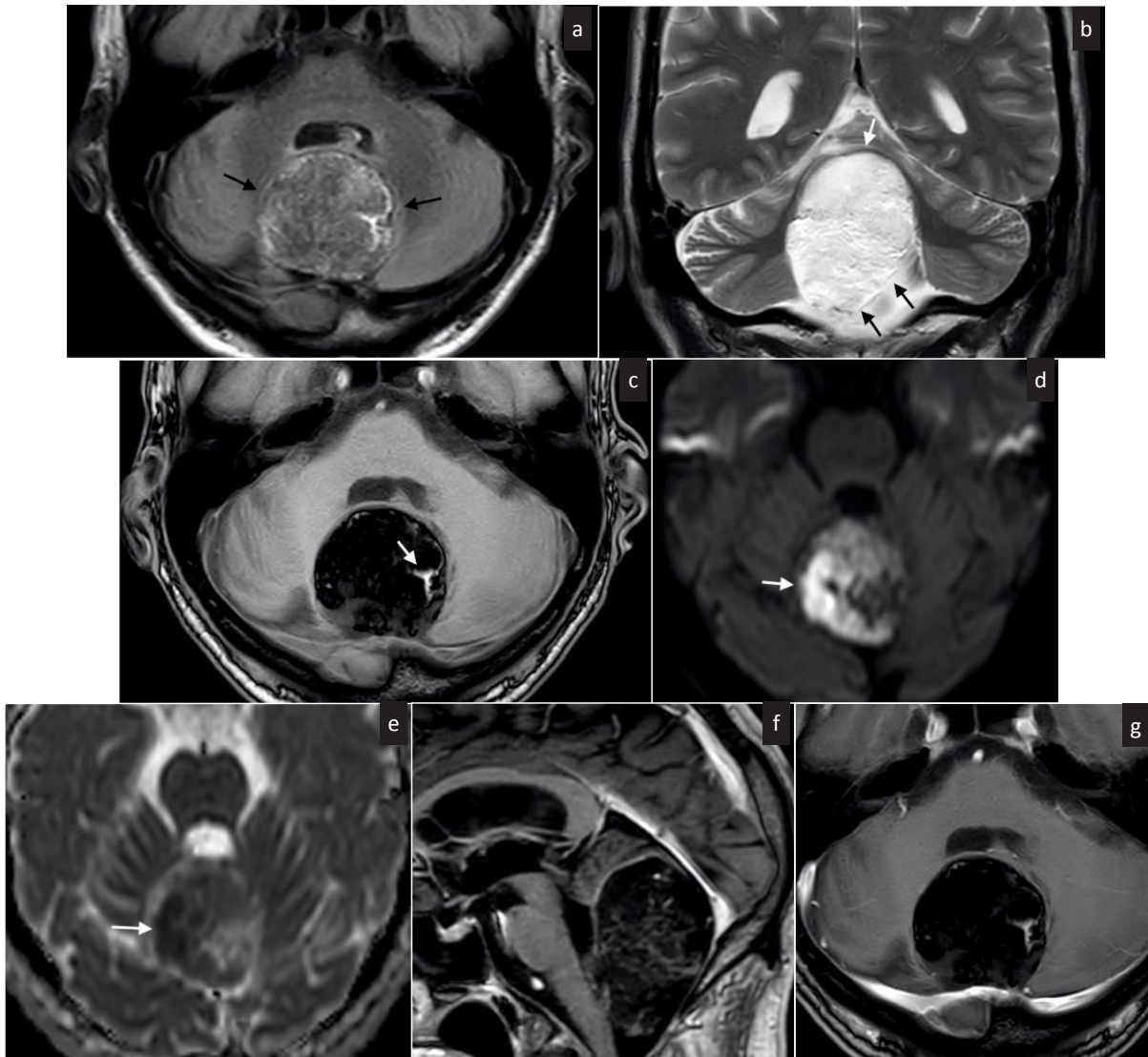


Fig. 11. Dermoid cyst of a 56-year-old male patient with headaches, tinnitus and vertigo. MRI scans show a large midline tumour in the posterior fossa with inhomogeneous FLAIR-signal (arrows in **a**) and hyperintense appearance on T2W image (arrows in **b**), with marked compression of the cerebellar parenchyma. The lesion contains T1-hyperintense fat inclusions (arrow in **c**), as well as components with restricted diffusion (arrows in **d**, **e**). The mass does not show significant contrast enhancement (**f**, **g**).

space-occupying, usually manifesting with headache and dizziness. On CT scans, the lesions appear isodense to CSF. On MRI, the cysts have a similar signal intensity to that of CSF in all sequences (**Fig. 9**). Rupture of an arachnoid cyst is extremely rare; however, in such cases, the isointense to CSF signal intensity is lost on FLAIR images due to haemorrhage within the cyst [24, 25].

Epidermoid cysts

Epidermoid cysts are comprised of a conglomerate of

horny scales, surrounded by an epidermal capsule, and account for 0.2-1% of all intracranial tumours. Due to their slow growth, they primarily affect adults. Intracranial epidermoid cysts occur in the CPA in 40% of cases and account for 5% of CPA tumours. Other common locations are the pineal and suprasellar regions, and the middle cranial fossa.

Imaging

On CT scans, epidermoid cysts present as lobulated, hy-

podense masses with typical localisation. Density values are comparable to those of a cyst. Occasionally, calcifications are found in the surrounding capsule components. Peripheral calcifications are found in 25% of cases. Since density values are similar to those of CSF, recognition of these extra-axial lesions may be difficult. Displacement of the surrounding brain structures can be the sole indication of an extra-axial lesion in native CT images.

MRI helps to confirm the diagnosis of an epidermoid cyst. Of great importance are FLAIR and diffusion-weighted sequences. Epidermoid cysts are hyperintense to CSF on FLAIR. On high b value diffusion-weighted MR sequences, they exhibit increased signal intensity and may thus be differentiated from dermoid cysts (**Fig. 10**). On conventional T1W and T2W sequences, signal intensity may be similar to that of CSF [20, 21, 26].

Dermoid cysts

Dermoid cysts contain fat, calcium, sweat glands, hair, as well as an epidermis. Intracranial dermoid cysts are less common than intracranial epidermoid cysts; however, they occur more frequently in the spine. They are mainly found in the posterior fossa, either within the vermis or in the fourth ventricle. Symptoms result

from displacement of CSF, chemical meningitis as a result of cyst rupture, and dissemination of cyst contents into the subarachnoid space.

Imaging

On CT scans, dermoid cysts appear with negative densities. They are extra-axial masses typically located in the midline. Enhancement after contrast administration is not usually observed. On MRI, dermoid cysts are hyperintense on T1W sequences and moderately hyperintense on T2W sequences (**Fig. 11**). Fat suppression can be applied to differentiate these lesions from haemorrhage [20, 21, 27, 28].

Conclusion

A wide range of differential diagnoses can be considered when an extra-axial lesion is present. The prognosis, follow-up, and treatment for extra-axial tumours vary and knowledge of their imaging characteristics and their clinical features assist in narrowing the differential diagnosis and optimising patient workup. **R**

Conflict of interest

The authors declared no conflicts of interest.

REFERENCES

1. Buetow M, Buetow P, Smirniotopoulos J. Typical, atypical and misleading features in meningioma. *Radiographics* 1991; 11: 1087-1106.
2. Rapalino O, Smirniotopoulos J. Extra-axial brain tumor. *Handb Clin Neurol* 2016; 135: 275-291.
3. Osborn AG. Extra-axial neoplasms, cysts and tumor-like lesions. In: Gourtsoyiannis NC, Ros PR (eds). *Radiologic-pathologic correlations from head to toe*. Springer, Berlin 2005, pp 27-33.
4. Germano IM, Edwards MSB, Davia RL, et al. Intracranial meningiomas of the first two decades of life. *J Neurosurg* 1994; 80: 447-453.
5. Louis DN, Scheithauer BW, Budka H, et al. In: Kleihues P, Cavenee WK (eds). *Pathology and genetics. Tumours of the nervous system. World Health Organization classification of tumours*. IARC Press, Lyon 2000.
6. Burger PC, Scheithauer BW. *Atlas of tumor pathology: tumors of the central nervous system*. AFIP, Washington 1994.
7. Louis DN, Perry A. The 2016 World Health Organization classification of tumors of the central nervous system: a summary. *Acta Neuropathol* 2016; 131(6): 803-820.
8. Zimmerman RD, Fleming CA, Saint-Louis LA, et al. Magnetic resonance imaging of meningiomas. *AJNR Am J Neuroradiol* 1985; 6(2): 149-157.
9. Lunardi P, Mastronardi L, Nardacci B, et al. "Dural tail" adjacent to acoustic neuroma on MRI: a case report. *Neuroradiology* 1993; 35(4): 270-271.
10. Politi M, Romeike BF, Papanagiotou P, et al. Intraosseous hemangioma of the skull with dural tail sign: radiologic features with pathologic correlation. *AJNR Am J Neuroradiol* 2005; 26(8): 2049-2052.

11. Drevelegas A, Karkavelas G, Chourmouzi D, et al. Meningeal tumors. In: Drevelegas A (ed). *Imaging of brain tumors with histological correlations*. Springer-Verlag, Berlin Heidelberg New York 2003, pp 177-214.
12. Tali ET, Yuh WTC, Nguyen HD. Cystic acoustic schwannoma: MR characteristics. *Am J Neuroradiol* 1993; 14: 1241-1247.
13. Fortnum H, O'Neill C, R Taylor R, et al. The role of magnetic resonance imaging in the identification of suspected acoustic neuroma: a systematic review of clinical and cost effectiveness and natural history. *Health Technol Assess* 2009; 13(18): iii-iv, ix-xi, 1-154.
14. Thamburaj K, Radhakrishnan VV, Thomas B, et al. Intratumoral microhemorrhages on T2*-weighted gradient-echo imaging helps differentiate vestibular schwannoma from meningioma. *AJNR Am J Neuroradiol* 2008; 29(3): 552-557.
15. Zealley IA, Cooper RC, Clifford KM, et al. MRI screening for acoustic neuroma: a comparison of fast spin echo and contrast enhanced imaging in 1233 patients. *Br J Radiol* 2000; 73(867): 242-247.
16. Casselman JW, Kuhweide R, Ampe W, et al. Pathology of the membranous labyrinth: comparison of T1- and T2-weighted and gadolinium-enhanced spin-echo and 3DFT-CISS imaging. *AJNR Am J Neuroradiol* 1993; 14: 59-69.
17. Jhaveri MD, Osborn AG, Salzman KL, et al. *Diagnostic Imaging Brain*, 3rd Edition Elsevier, Philadelphia 2015.
18. Yousem DM, Patrone MP, Grossman RI. Leptomeningeal metastasis: MR evaluation. *J Comput Assist Tomogr* 1990; 14: 255-261.
19. Patronas NJ. Brain metastasis. In: Drevelegas A (ed). *Imaging of brain tumors with histological correlations*. Springer-Verlag, Berlin Heidelberg 2003, pp 373-399.
20. Drevelegas A. Extra-axial brain tumors. *Eur Radiol* 2005; 15(3): 453-467.
21. Papanagiotou P, Ketter R, Reith W. Extra-axial brain tumors. *Radiologe* 2012; 528129.b1129-1146.
22. Chourmouzi D, Potsi S, Moutzouoglou A, et al. Dural lesions mimicking meningiomas: A pictorial essay. *World J Radiol* 2012; 4(3): 75-82.
23. Goldberg HI. Extraaxial brain tumors. In: Atlas SW (ed). *MRI of the brain and spine*. Raven Press 1991, pp 352- 353.
24. Tsitsopoulos P, Pantazis GC, Syrmou EC, et al. Intracranial arachnoid cyst associated with traumatic intracystic hemorrhage and subdural haematoma. *Hippokratia* 2008; 12(1): 53-55.
25. Awaji M, Okamoto K, Nishiyama K, al. Magnetic resonance cisternography for preoperative evaluation of arachnoid cysts. *Neuroradiology* 2007; 49(9): 721-726.
26. Horowitz BL, Chari MV, James R, et al. MR of intracranial epidermoid tumors: correlation of in vivo imaging with in vitro 13C spectroscopy. *AJNR Am J Neuroradiol* 1990; 11(2): 299-302.
27. Smith AS, Benson JE, Blaser SI, et al. Diagnosis of ruptured intracranial dermoid cyst: value MR over CT. *AJNR Am J Neuroradiol* 1991; 12(1): 175-180.
28. Politi M, Papanagiotou P. Tumors of the posterior cranial fossa. *Radiologe* 2016; 56(11): 967-975.



READY - MADE
CITATION

Politi M, Alektorov K, Mouloupoulos LA, Papanagiotou P. Extra-axial brain tumours and cysts. *Hell J Radiol* 2020; 5(3): 30-42.